

As a library, NLM provides access to scientific literature. Inclusion in an NLM database does not imply endorsement of, or agreement with, the contents by NLM or the National Institutes of Health.

Learn more: [PMC Disclaimer](#) | [PMC Copyright Notice](#)

## Author Manuscript

Peer reviewed and accepted for publication by a journal



*J Musculoskelet Neuronal Interact*. Author manuscript; available in PMC: 2015 Nov 20.

*Published in final edited form as:* *J Musculoskelet Neuronal Interact*. 2013 Dec;13(4):405–411.

# Spaceflight and hind limb unloading induce similar changes in electrical impedance characteristics of mouse gastrocnemius muscle

[M Sung](#)<sup>1</sup>, [J Li](#)<sup>1</sup>, [AJ Spieker](#)<sup>1</sup>, [J Spatz](#)<sup>2</sup>, [R Ellman](#)<sup>2</sup>, [VL Ferguson](#)<sup>3</sup>, [TA Bateman](#)<sup>4</sup>, [GD Rosen](#)<sup>1</sup>, [M Bouxsein](#)<sup>2</sup>, [SB Rutkove](#)<sup>1</sup>

[Author information](#) [Copyright and License information](#)

PMCID: PMC4653813 NIHMSID: NIHMS549401 PMID: [24292610](#)

## Abstract

---

### Objective

To assess the potential of electrical impedance myography (EIM) to serve as a marker of muscle fiber atrophy and secondarily as an indicator of bone deterioration by assessing the effects of spaceflight or hind limb unloading.

### Methods

In the first experiment, 6 mice were flown aboard the space shuttle (STS-135) for 13 days and 8 earthbound mice served as controls. In the second experiment, 14 mice underwent hind limb unloading (HLU) for 13 days; 13 additional mice served as controls. EIM measurements were made on *ex vivo* gastrocnemius muscle. Quantitative microscopy and areal bone mineral density (aBMD) measurements of the hindlimb were also performed.

## Results

Reductions in the multifrequency phase-slope parameter were observed for both the space flight and HLU cohorts compared to their respective controls. For ground control and spaceflight groups, the values were  $24.7 \pm 1.3^\circ/\text{MHz}$  and  $14.1 \pm 1.6^\circ/\text{MHz}$ , respectively ( $p=0.0013$ ); for control and HLU groups, the values were  $23.9 \pm 1.6^\circ/\text{MHz}$  and  $19.0 \pm 1.0^\circ/\text{MHz}$ , respectively ( $p=0.014$ ). This parameter also correlated with muscle fiber size ( $\rho=0.65$ ,  $p=0.011$ ) for spaceflight and hind limb aBMD ( $\rho=0.65$ ,  $p=0.0063$ ) for both groups.

## Conclusions

These data support the concept that EIM may serve as a useful tool for assessment of muscle disuse secondary to immobilization or microgravity.

**Keywords:** Muscle, Spaceflight, Hind Limb Unloading, Disuse, Electrical Impedance

## Introduction

---

Exposure to prolonged disuse or microgravity produces a variety of effects on skeletal muscle, including fiber atrophy, a reduction in maximal force, and reduced endurance<sup>1</sup>. For example, given the major alterations that can ensue even after just several days of exposure to microgravity, human spaceflight currently requires astronauts to participate in daily exercise countermeasures to help offset the effects of weightlessness<sup>2</sup>. Although a recent report suggests that high intensity exercise combined with optimal nutrition may mitigate bone and muscle loss<sup>3</sup>, novel approaches to reduce negative effects of spaceflight or prolonged bed rest/immobilization on musculoskeletal health, including drug therapies, are being sought<sup>4,5</sup>.

Diagnostic tools for the assessment of muscle and bone loss due to disuse or weightlessness are, however, quite limited. Standard methods used to evaluate these changes such as dual-energy X-ray absorptiometry (DXA) and quantitative computed tomography<sup>6,7</sup> are expensive and inconvenient for regular clinical use. Moreover, they are not feasible in spaceflight, given the size, weight, and power requirements of the equipment. Ultrasound is being studied for muscle loss assessment in spaceflight, but quantifying the measurements requires substantial procedural modification<sup>8</sup>. Simple force-testing dynamometers are inconvenient and inaccurate to use on debilitated patients and are virtually impossible to use in space. For these reasons, other non-invasive approaches that can be applied easily and rapidly to both patients and astronauts are of interest. One approach that offers potential value is electrical impedance myography (EIM). EIM is a technique in which a high-frequency, low-energy electrical current is applied to a localized area of muscle and the resulting surface voltages are measured<sup>9</sup>. EIM is a specialized version of methods developed in the well-studied field of bioelectrical impedance spectroscopy, in which alterations in the characteristics of a tissue or cellular suspension are

characterized by their electrical frequency-dependent properties<sup>10-13</sup>. In addition to these non-muscular studies, at least one investigation has evaluated the specific relationship between muscle cell size and bioimpedance parameters in tissue culture<sup>14</sup>.

Since the EIM technique is painless, rapid to apply, non-invasive, and the equipment lightweight, it has the potential to serve as a useful method for monitoring muscle status. Earlier studies have shown that surface EIM alterations are closely tied to muscle fiber size<sup>15</sup>. Importantly, data in humans<sup>16</sup> and in rats<sup>17</sup> support that EIM is sensitive to changes in muscle following disuse, with reductions in EIM parameters of greater than 30% from baseline, and thus may also have the potential to sensitively identify the impact of disuse or microgravity on muscle health. Here we further explore the potential application of EIM for the assessment of muscle impacted by disuse by studying *ex vivo* muscle obtained from mice exposed to reduced mechanical loading via hind limb unloading (HLU) or spaceflight, testing the basic hypothesis that such disuse will consistently alter EIM values.

## Materials and methods

---

### Animals

For both the hind limb unloading (HLU) and spaceflight experiments, we used 9-week-old female C57Bl/6N mice (Charles River, Wilmington, MA). In the HLU cohort, 13 ground control and 14 HLU mice were studied, while in the space flight study, 8 ground control and 6 space flight mice were examined. The HLU protocol was approved by Beth Israel Deaconess Medical Center's Institutional Animal Care and Use Committee (IACUC), and the protocol used for the spaceflight study was approved by the ACUC at Kennedy Space Center.

### Spaceflight study

Both spaceflight and ground control animals were maintained on a NASA nutrient-upgraded rodent food bar<sup>18</sup> throughout the experiment. Spaceflight animals were sacrificed within approximately 2.5-7.5 hours of the shuttle's completing a 12 day, 18.5 hour flight on board the shuttle *Atlantis* (STS-135 mission). Flight animals were euthanized and the right gastrocnemius muscle was removed intact. Ground control animals, matched to day 0 body weight and bone parameters of flight mice, were euthanized 2 days later and the gastrocnemius muscle removed in an identical fashion, after an equal length of stay in identical cages to those used on the space shuttle<sup>19</sup>.

### Hind Limb Unloading studies

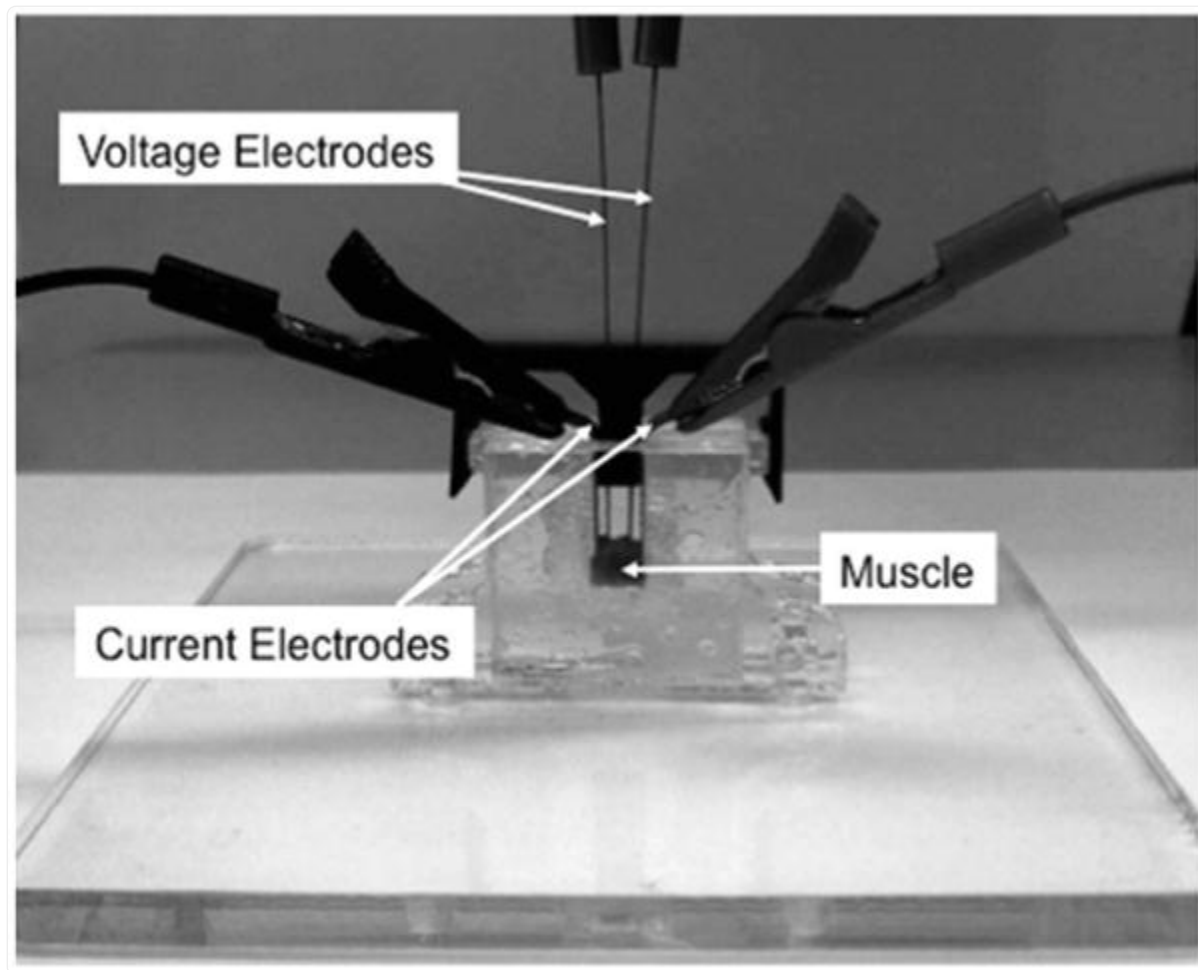
In a later experiment, mice of the same strain, sex and age were subjected to HLU for 13 days and compared to concurrent normally-loaded controls<sup>20</sup>. Briefly, under isoflurane anesthesia, the tail was taped to a freely rotating

harness connected to a wheel that could move along a rod across the center of the cage. The height of the harness was adjusted such that the mouse could not touch its hind paws to the floor. A reloading period of 3 to 6 hours, to match the STS-135 timing, was employed in the HLU group by removing the harness and allowing the mice to ambulate before sacrifice. NASA food bars and water were provided *ad libitum*.

## Muscle processing and electrical impedance measurements

Excised muscle was immediately weighed and then cut to a  $0.5\text{ cm} \times 0.5\text{ cm}$  base with approximately a  $0.3\text{ cm}$  height block using a razor blade. The block of muscle tissue was placed in a  $0.5\text{ cm} \times 0.5\text{ cm}$  base impedance-measuring cell ([Figure 1](#)), configured with two broad, stainless steel electrodes on two sides for applying electrical current and two needle electrodes positioned on top for measuring voltage, as previously described<sup>15</sup>. The impedance data were obtained using the Imp SFB7<sup>®</sup> (Impedimed, San Diego, CA). Reactance (X) and resistance (R) data from 3 to 500 kHz was collected. The muscle was placed such that electrical current would flow across (transversely) to the major muscle fiber direction. While it would have been preferable to also obtain measurements with electrical current flow parallel to the fibers (and thus allowing us to assess the anisotropic characteristics of the tissue), positioning the muscle fibers on end with the metal plate electrodes proved very challenging. A preliminary review of the data showed this latter process to be quite inconsistent, and thus was omitted from any further analysis.

Figure 1.



[Open in a new tab](#)

Impedance measuring cell with muscle demonstrating how data was obtained.

## Muscle histology (obtained on space flight muscle only)

Immediately after the EIM data were collected, the muscle was snap-frozen in isopentane cooled in liquid nitrogen, and stored at  $-80^{\circ}\text{C}$ . The tissue was then cut into  $10\text{ }\mu\text{m}$  slices using a Tissue Tek II cryostat (Miles Laboratories, Inc., Elkhart, IN) and stained with hematoxylin and eosin. Cell measurements were made using a Zeiss Axiophot microscope with a LUDL motorized stage interfaced with a Dell Optiflex 380 computer running Stereo Investigator (MBF Biosciences, Inc., Williston, VT) software. This software allows a non-biased quantification of fiber sizes. After the investigator sets a series of initial parameters, including the section of tissue from which to choose cells, the system

automatically and randomly selects groups of cells to count. Approximately 60 cells were evaluated from each animal. In order to reduce the potential for any bias, the evaluator (AS) was blinded to group designation (i.e., loaded or unloaded) of each section being assessed. Muscle histology was also planned in the HLU animals, but unfortunately the tissue was inadvertently damaged during transport and was unusable for analysis.

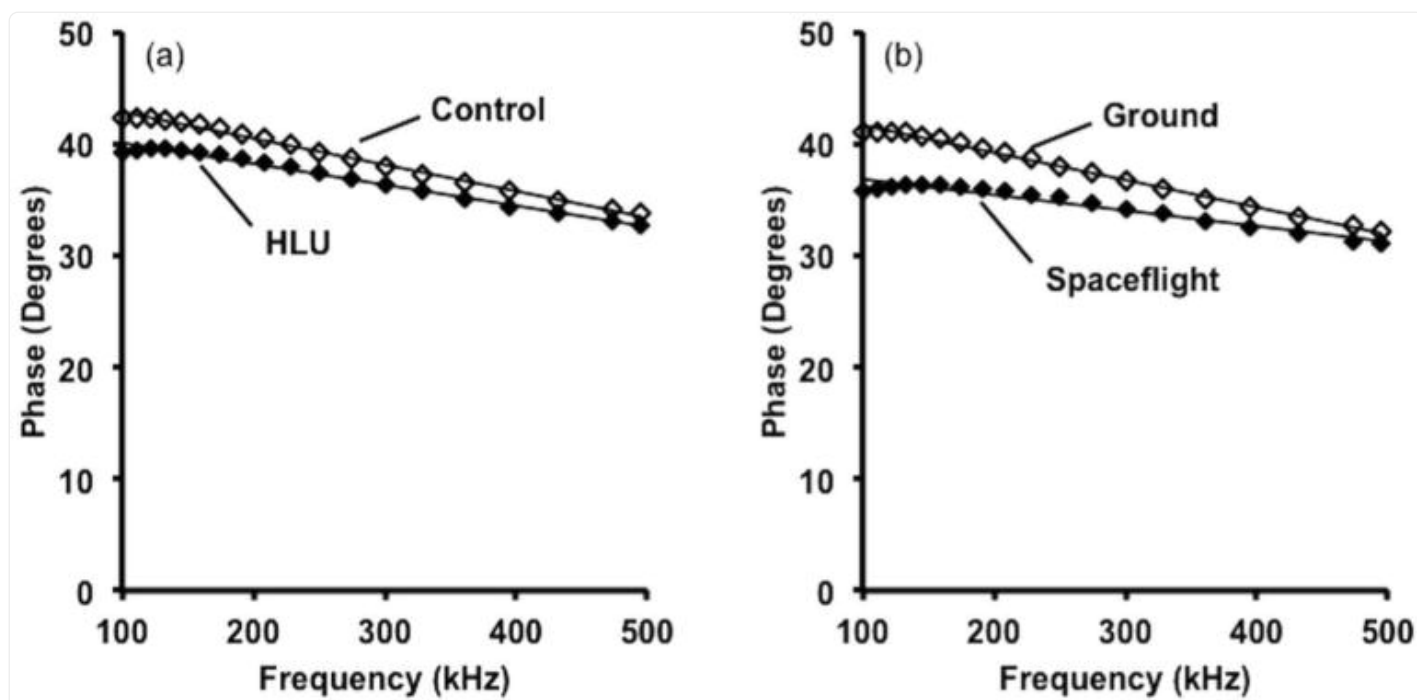
## Bone Mineral Density measurements

Areal bone mineral density (aBMD,  $\text{g}/\text{cm}^2$ ) of the hind limb (from femoral neck to ankle) was assessed by peripheral dual-energy X-ray absorptiometry (pDXA, PIXImus II; GE Lunar, Madison, WI, USA) *in vivo* immediately prior to sacrifice.

## Data analysis

From the raw EIM data, the phase was calculated via the equation:  $\text{phase} = \arctan(\text{reactance}/\text{resistance})$  at each frequency. Due to its being the most promising of the multifrequency EIM parameters from previous work<sup>[21,22](#)</sup>, and especially in our recent work in HLU<sup>[17](#)</sup> rats, the focus here is on the phase-slope parameter, defined as the slope of the fitted linear regression to phase values from 100 to 500 kHz (see [Figure 2](#) for examples as to how this analysis was performed), expressed as degrees/MHz. Although considerably beyond the 50 kHz measurement, the subject much earlier work, the impedance behavior in this region is generally linear and thus favorable to least squares regression analysis. For simplicity of description, the sign was then flipped (thus the negative values are positive). Further explanation as to the potential significance of this parameter is provided in the discussion.

Figure 2.



[Open in a new tab](#)

Plots of the average phase from a hind limb unloaded mouse and spaceflight mouse with controls. Dotted lines depict the method of calculating the 100-500 kHz phase-slope parameter.

The Wilcoxon rank sum test was performed to evaluate for differences between phase-slope, muscle mass, muscle fiber cross-sectional area, and areal bone mineral density of the HLU and space flight mice with their respective control groups. Spearman rank-correlation coefficient ( $\rho$ ) was calculated to determine the relationship between phase-slope and muscle mass, muscle fiber area, and hind limb bone mineral density. All results are given as mean  $\pm$  standard error; significance was assumed at  $p < 0.05$ , two-tailed.

## Results

### Muscle mass

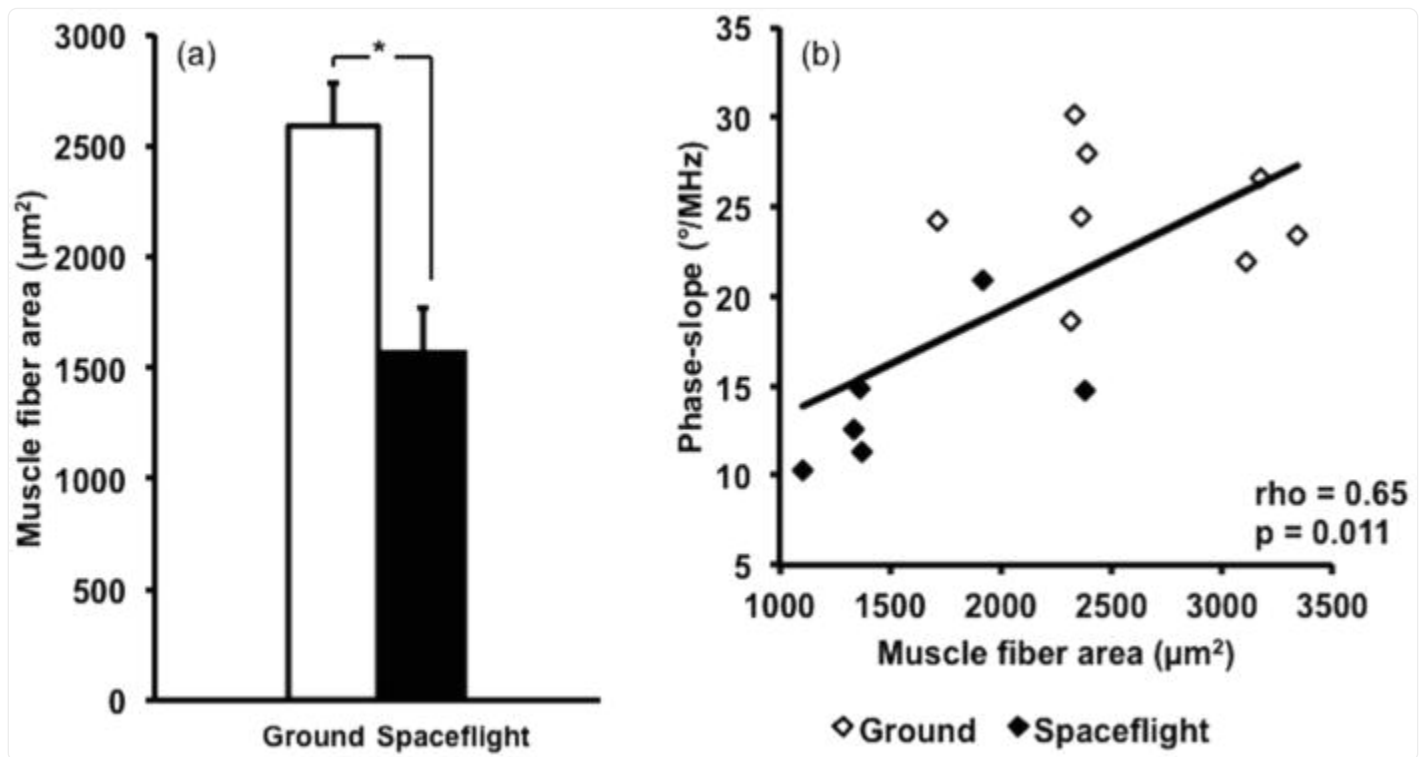
As anticipated, mice exposed to spaceflight had a lower gastrocnemius muscle mass than ground controls, although the difference did not reach significance ( $102 \pm 32$  mg for spaceflight;  $112 \pm 22$  mg for ground  $p = 0.079$ ). However, mice

exposed to HLU had lower muscle mass as compared to controls ( $95.2 \pm 19$  mg for HLU;  $107 \pm 29$  mg for control;  $p=0.0053$ ).

## Muscle fiber size (spaceflight only)

Muscle histology measurements were obtained only in the spaceflight animals and their controls. As anticipated, mice exposed to spaceflight had a smaller average muscle fiber cross-sectional area of  $1579 \pm 194 \mu\text{m}^2$  as compared to  $2591 \pm 197 \mu\text{m}^2$  in controls ( $p=0.013$ ) ([Figure 3 \(a\)](#)).

Figure 3.



[Open in a new tab](#)

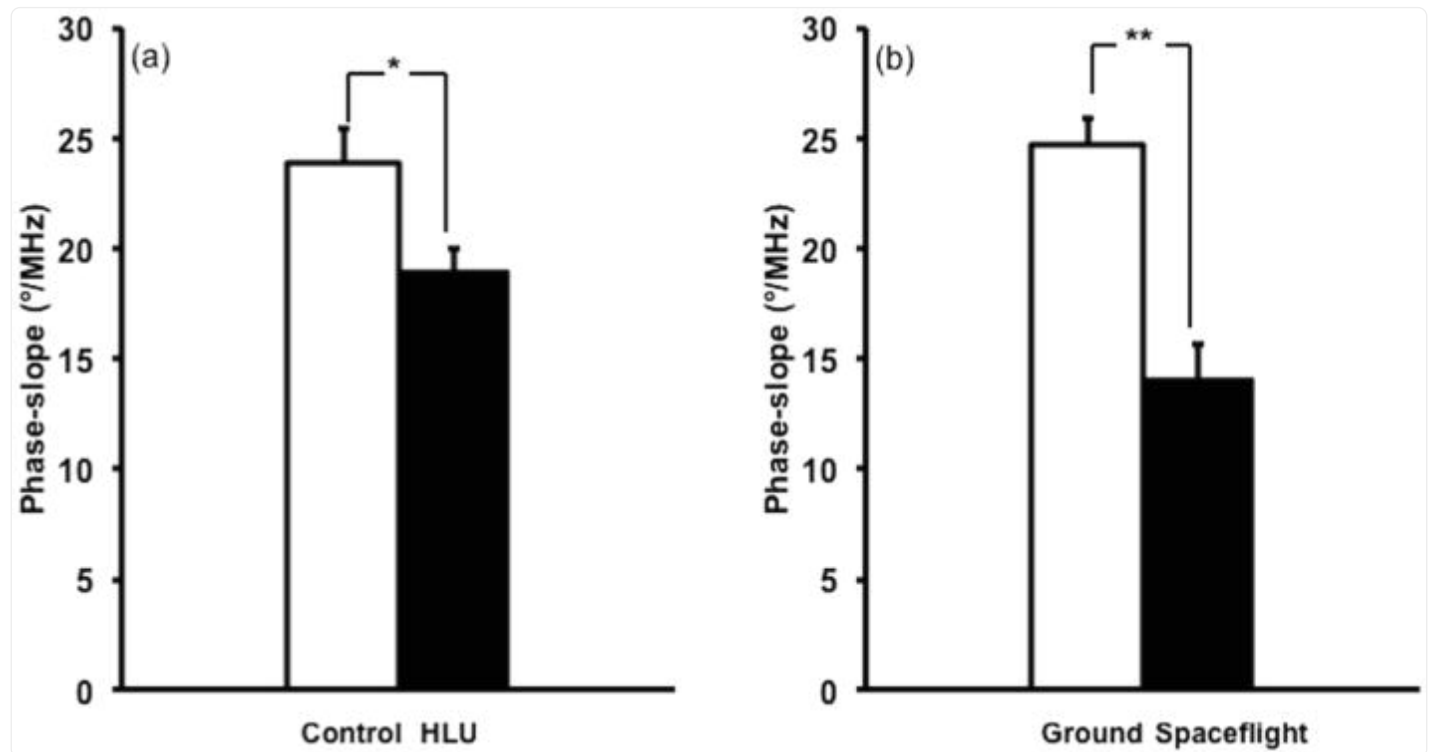
(a). Column plot of average muscle fiber size in ground vs. space flight mice. (b) Scatter plot correlating phase-slope and average muscle fiber size in ground and space flight mice.

## Electrical Impedance data and muscle characteristics



The EIM phase-slope parameter was significantly lower in both the spaceflight and HLU mice when compared to their respective control groups ([Figure 4](#)). For control and HLU groups, the values were  $23.9 \pm 1.6^\circ/\text{MHz}$  and  $19.0 \pm 1.0^\circ/\text{MHz}$ , respectively ( $p=0.014$ ); for ground control and spaceflight groups, the values were  $24.7 \pm 1.3^\circ/\text{MHz}$  and  $14.1 \pm 1.6^\circ/\text{MHz}$ , respectively ( $p=0.0013$ ). We observed a moderate positive relationship between muscle mass and the EIM phase-slope parameter in the HLU study ( $\rho=0.64$ ,  $p<0.001$ ), and although the relationship had a similar pattern in the spaceflight study, the association was weaker and did not reach statistical significance ( $\rho=0.39$ ,  $p=0.17$ ) ([Figure 5](#)). This inconsistency may relate to the fact that there were considerably smaller number of spaceflight animals and that muscle mass was slightly lower in the HLU group than the spaceflight group compared to their respective control groups. However, there was a good correlation between muscle fiber size and the phase-slope parameter ( $\rho=0.65$ ,  $p=0.011$ ) across the spaceflight and ground control animals ([Figure 3 \(b\)](#)).

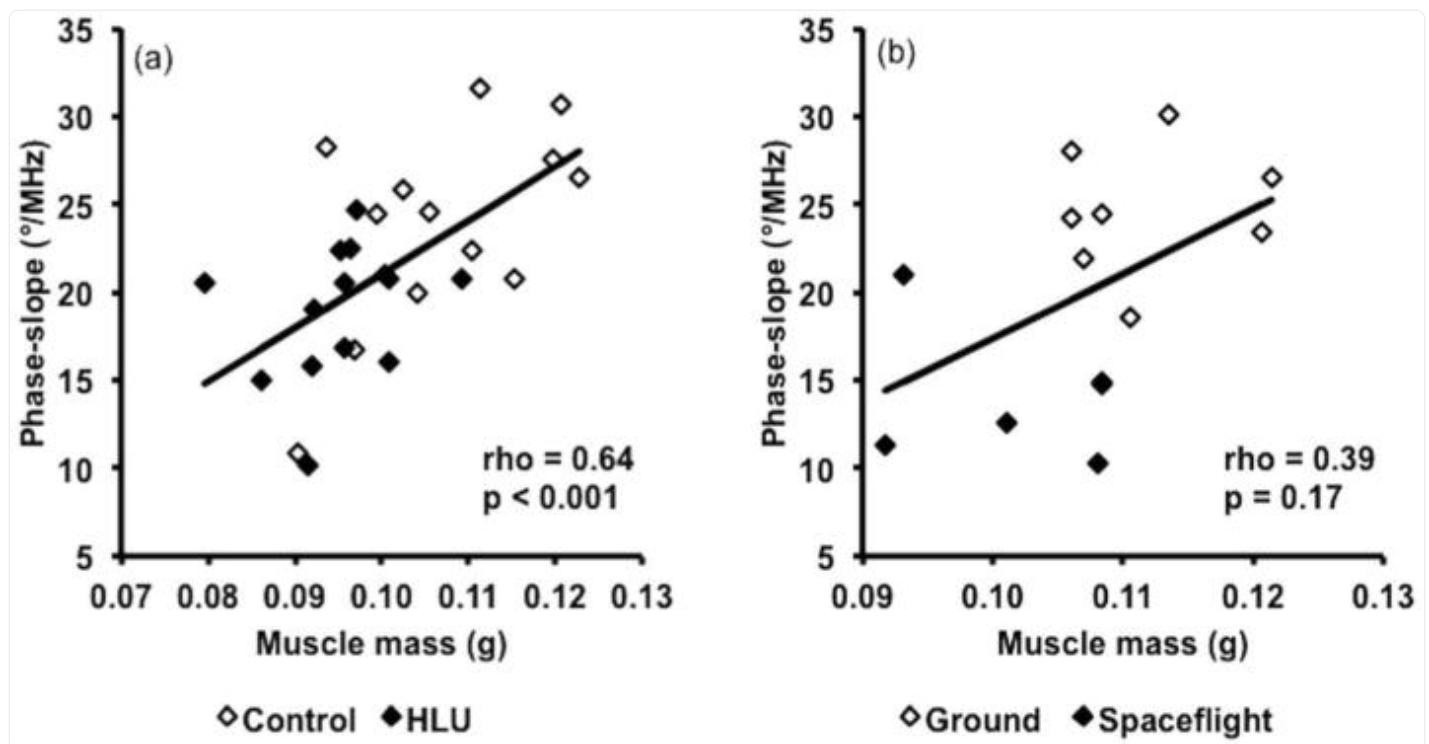
Figure 4.



[Open in a new tab](#)

Column plot depicting the average phase-slope of controls vs. hind limb unloaded mice (a) and ground vs. space flight animals (b).

Figure 5.



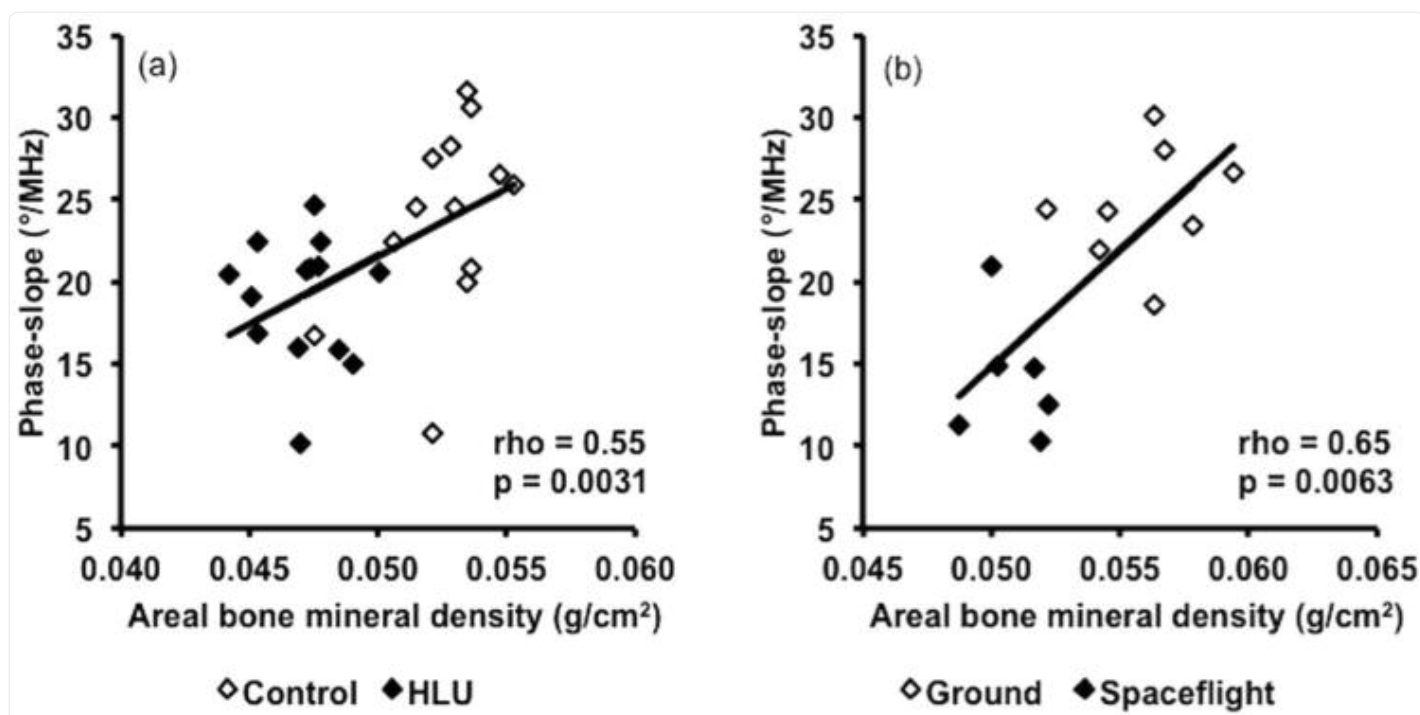
[Open in a new tab](#)

Scatter plots correlating phase-slope and muscle mass in control and hind limb unloaded mice (a) and control and space flight mice (b).

## Areal Bone Mineral Density and Electrical Impedance

As expected, both spaceflight and HLU groups had significantly lower hind limb aBMD compared to controls. For ground control and spaceflight groups, the values were  $55.9 \pm 0.80 \times 10^{-3} \text{ g/cm}^2$  and  $50.8 \pm 0.56 \times 10^{-3} \text{ g/cm}^2$ , respectively ( $p=0.0013$ ). For control and HLU groups, the values were  $52.6 \pm 0.55 \times 10^{-3} \text{ g/cm}^2$  and  $47.1 \pm 0.44 \times 10^{-3} \text{ g/cm}^2$ , respectively ( $p<0.001$ ). In both studies, there were significant correlations between hind limb aBMD and the phase-slope parameter, both assessed using aBMD and EIM values obtained at the end of the study (HLU study:  $\rho=0.55$ ,  $p=0.0031$  and space flight study:  $\rho=0.65$ ,  $p=0.0063$ , [Figure 6](#)).

Figure 6.



[Open in a new tab](#)

Scatter plots correlating phase-slope and areal bone mineral density in control and hind limb unloaded mice (a) and control and space flight mice (b).

## Discussion

These results support the hypothesis that significant alterations in the electrical impedance of mouse muscle occur after exposure to both spaceflight and hind limb unloading, consistent with our earlier *in vivo* observations seen in humans following disuse due to casting<sup>16</sup> and rats undergoing hind limb unloading<sup>17</sup>. Moreover, these EIM alterations correlate with muscle fiber size and also to hind limb aBMD. The consistency of the majority of these results in the two separate experiments supports their authenticity. Thus, the EIM changes observed here likely reflect true alterations to the composition and structure of the muscle tissue itself, including reductions in muscle fiber size and possibly the deposition of connective tissue<sup>23</sup>.

The major outcome measure we have utilized here, the phase-slope, as its derivation described in [Figure 2](#) shows, is a measure of the frequency-dependence of the impedance<sup>21</sup>. Muscle can be modeled as a complex network of resistors

and capacitors<sup>24</sup>. At these frequencies of applied current, the extracellular space serves as the major resistive component and the sarcolemma of the cell membranes serves as the major capacitive component. The resulting voltages from such complex circuits are typically very sensitive to current frequency and thus even subtle alterations in the structure and composition of the tissue are likely to be observed as shifts in the phase-slope measurement. The phase itself represents a combination of both the resistive and reactive elements in the circuit and has been shown to be very sensitive to a variety of neuromuscular diseases as well as to disuse atrophy<sup>16,21,25,26</sup>. Taken together, the changes in the phase-slope measure likely represent a reduction in overall surface area of sarcolemmal membrane due to reduced muscle fiber area, as supported by our quantitative microscopy data. Such reduced fiber area would likely be associated with reduced muscle contractile force and power<sup>27</sup>.

Importantly, the alterations observed in the EIM data correlated with meaningful and potentially important measures, including muscle fiber size and, very preliminarily, hind limb aBMD. Previous studies have already identified EIM data correlating significantly to muscle fiber size in rats, in both sciatic crush and HLU models<sup>15,17</sup>. However, this is the first time that a relationship between EIM and aBMD has been suggested. Since muscle contractions provide much of the mechanical loading experienced by bone, and prior studies have shown associations between muscle mass and aBMD<sup>28</sup>, it is perhaps not surprising that calf muscle EIM measurements correlate with leg aBMD. Longitudinal measurements of muscle mass, EIM, and bone mass would allow a better understanding of the temporal relationship between bone and muscle changes in response to disuse.

The gastrocnemius was studied in these two experiments. Previous studies have shown that in rodents, type 1 muscle fibers tend to atrophy more than type 2 fibers during spaceflight<sup>29,30</sup>. Thus, the soleus, which consists mainly of type 1 fibers, generally shows greater alteration than the gastrocnemius which mostly consists of type 2 fibers<sup>31</sup>. Still, some alteration in the gastrocnemius muscle does occur, and it is reassuring that measurement of this less affected muscle still identified a change following disuse. The soleus was not studied for two major reasons. First, the soleus from the spaceflight experiment was not available to this group of researchers. Second, the mouse soleus is considerably smaller than the gastrocnemius and would have been technically challenging to work with and measure *ex vivo* in the impedance measurement cell even had it been available.

There are several limitations to this study worth highlighting, most of which relate to the study design. First, no *in vivo* EIM measurements were made. One of the potentially most important aspects of EIM is its ability to measure and quantify muscle health rapidly and non-invasively. Thus, it would be valuable to monitor *in vivo* surface EIM change longitudinally, as was done in the study on rats<sup>17</sup>, and to correlate *in vivo* EIM data with *in vivo* bone mass data, as well as to *ex vivo* muscle histology and bone microarchitecture. Second, we did not perform any functional testing of the muscle unit or muscle fibers, which would have allowed us to relate dynamic changes to the EIM data. Third, the impedance-measuring device used here (the Imp SFB7<sup>®</sup> from Impedimed, Inc) is limited in that it is not specifically designed for this use, having been developed for whole-body bioimpedance analysis measurements. It is likely that a dedicated muscle impedance-measuring device would have offered even greater sensitivity to these changes. Fourth, it

is possible that the DXA measurements were impacted by the muscle loss to some extent; ideally, qCT measurements would have been performed to more accurately assess bone mineral density. Finally, it is impossible to exclude the possibility that water shifts or dehydration from prolonged suspension/spaceflight may be contributing to the observed changes in the EIM parameters. Although in both experiments the animals were allowed to locomote normally for a period of time before necropsy, simple shifts in muscle water content could have influenced the EIM results. We do note, however, that other work has shown no evidence of impedance change even with 23% reduction in total body weight over a 48-hour period of water restriction (unpublished results, Rutkove and Li, 2013).

In summary, we have identified similar alterations in the electrical impedance of muscle after exposure to either microgravity or hind limb unloading and these alterations correlate with both muscle fiber size (in space flight animals) and hind limb aBMD. These results support the need for further study of EIM technology for use in *in vivo* monitoring of muscle alteration during spaceflight and other conditions leading to musculoskeletal disuse.

## Acknowledgments

---

This work was funded by NASA grant NNX10AE39G. Additional funding for the STS-135 experiment was provided by NASA NNJ10GA25A; NSBRI MA00002 and BL01302; Amgen/UCB Pharma; and BioServe Space Technologies at the University of Colorado, Boulder CO.

## Footnotes

---

Dr. Rutkove has equity in, and serves a consultant and scientific advisor to Skulpt, Inc. a company that designs impedance devices for clinical and research use; he is also a member of the company's Board of Directors. The company also has an option to license patented impedance technology of which Dr. Rutkove is named as an inventor. This study, however, did not employ any relevant company or patented technology.

## References

---

1. Tischler ME, Slentz M. Impact of weightlessness on muscle function. ASGSB Bull. 1995;8:73–81. [[PubMed](#)] [[Google Scholar](#) ]
2. Convertino VA, Sandler H. Exercise countermeasures for spaceflight. Acta Astronaut. 1995;35:253–70. doi: 10.1016/0094-5765(95)98731-n. [[DOI](#) ] [[PubMed](#)] [[Google Scholar](#) ]
3. Smith SM, Heer MA, Shackelford LC, Sibonga JD, Ploutz-Snyder L, Zwart SR. Benefits for bone from resistance exercise and nutrition in long-duration spaceflight: Evidence from biochemistry and densitometry. J

Bone Miner Res. 2012;27:1896–906. doi: 10.1002/jbmr.1647. [[DOI](#)] [[PubMed](#)] [[Google Scholar](#)]

4. Leblanc A, Matsumoto T, Jones J, et al. Bisphosphonates as a supplement to exercise to protect bone during long-duration spaceflight. Osteoporos Int. 2013;24:2105–14. doi: 10.1007/s00198-012-2243-z. [[DOI](#)] [[PubMed](#)] [[Google Scholar](#)]

5. Wimalawansa SM, Wimalawansa SJ. A novel pharmacological approach of musculoskeletal losses associated with simulated microgravity. J Musculoskelet Neuronal Interact. 2000;1:35–41. [[PubMed](#)] [[Google Scholar](#)]

6. LeBlanc A, Schneider V, Shackelford L, et al. Bone mineral and lean tissue loss after long duration space flight. J Musculoskelet Neuronal Interact. 2000;1:157–60. [[PubMed](#)] [[Google Scholar](#)]

7. Lang T, LeBlanc A, Evans H, Lu Y, Genant H, Yu A. Cortical and trabecular bone mineral loss from the spine and hip in long-duration spaceflight. J Bone Miner Res. 2004;19:1006–12. doi: 10.1359/JBMR.040307. [[DOI](#)] [[PubMed](#)] [[Google Scholar](#)]

8. Scott JM, Martin DS, Ploutz-Snyder R, et al. Reliability and validity of panoramic ultrasound for muscle quantification. Ultrasound Med Biol. 2012;38:1656–61. doi: 10.1016/j.ultrasmedbio.2012.04.018. [[DOI](#)] [[PubMed](#)] [[Google Scholar](#)]

9. Rutkove SB. Electrical Impedance Myography: Background, Current State, and Future Directions. Muscle Nerve. 2009;40:936–46. doi: 10.1002/mus.21362. [[DOI](#)] [[PMC free article](#)] [[PubMed](#)] [[Google Scholar](#)]

10. Grimnes S, Martinsen OG. Bioimpedance and Bioelectricity Basics. Second. London: Academic press; 2008. [[Google Scholar](#)]

11. Schwan HP. Electrical properties of tissue and cell suspensions. Adv Biol Med Phys. 1957;5:147–209. doi: 10.1016/b978-1-4832-3111-2.50008-0. [[DOI](#)] [[PubMed](#)] [[Google Scholar](#)]

12. Schwan HP. Mechanisms responsible for electrical properties of tissues and cell suspensions. Med Prog Technol. 1993;19:163–5. [[PubMed](#)] [[Google Scholar](#)]

13. Ackmann JJ. Complex bioelectric impedance measurement system for the frequency range from 5 Hz to 1 MHz. Ann Biomed Eng. 1993;21:135–46. doi: 10.1007/BF02367609. [[DOI](#)] [[PubMed](#)] [[Google Scholar](#)]

14. Rakhilin S, Turner G, Katz M, et al. Electrical impedance as a novel biomarker of myotube atrophy and hypertrophy. J Biomol Screen. 2011;16:565–74. doi: 10.1177/1087057111401392. [[DOI](#)] [[PubMed](#)] [[Google Scholar](#)]

15. Ahad MA, Fogerson PM, Rosen GD, Narayanswami P, Rutkove SB. Electrical characteristics of rat skeletal muscle in immaturity, adulthood, and after sciatic nerve injury and their relation to muscle fiber size.

Physiol Meas. 2009;30:1415–27. doi: 10.1088/0967-3334/30/12/009. [[DOI](#)] [[PMC free article](#)] [[PubMed](#)] [[Google Scholar](#)]

16. Tarulli AW, Duggal N, Esper GJ, et al. Electrical impedance myography in the assessment of disuse atrophy. Arch Phys Med Rehabil. 2009;90:1806–10. doi: 10.1016/j.apmr.2009.04.007. [[DOI](#)] [[PMC free article](#)] [[PubMed](#)] [[Google Scholar](#)]

17. Li J, Spieker AJ, Rosen GD, Rutkove SB. Electrical impedance alterations in the rat hind limb with unloading. J Musculoskelet Neuronal Interact. 2013;13(1):37–44. [[PMC free article](#)] [[PubMed](#)] [[Google Scholar](#)]

18. Sun GS, Tou JC, Liittschwager K, et al. Evaluation of the nutrient-upgraded rodent food bar for rodent spaceflight experiments. Nutrition. 2010;26:1163–9. doi: 10.1016/j.nut.2009.09.018. [[DOI](#)] [[PubMed](#)] [[Google Scholar](#)]

19. Dalton P, Gould M, Girten B, Stodieck LS, Bateman TA. Preventing annoyance from odors in spaceflight: a method for evaluating the sensory impact of rodent housing. Journal of applied physiology. 2003;95:2113–21. doi: 10.1152/jappphysiol.00399.2003. [[DOI](#)] [[PubMed](#)] [[Google Scholar](#)]

20. Riley D, Slocum G, Bain J, Sedlak F, Sowa T, Mellender J. Rat hindlimb unloading: soleus histochemistry, ultrastructure, and electromyography. J Appl Physiol. 1990;69:58–66. doi: 10.1152/jappl.1990.69.1.58. [[DOI](#)] [[PubMed](#)] [[Google Scholar](#)]

21. Rutkove SB, Shefner JM, Gregas M, et al. Characterizing spinal muscular atrophy with electrical impedance myography. Muscle Nerve. 2010;42:915–21. doi: 10.1002/mus.21784. [[DOI](#)] [[PubMed](#)] [[Google Scholar](#)]

22. Wang LL, Spieker AJ, Li J, Rutkove SB. Electrical impedance myography for monitoring motor neuron loss in the SOD1 G93A amyotrophic lateral sclerosis rat. Clin Neurophysiol. 2011;122:2505–11. doi: 10.1016/j.clinph.2011.04.021. [[DOI](#)] [[PMC free article](#)] [[PubMed](#)] [[Google Scholar](#)]

23. Jarvinen TA, Jozsa L, Kannus P, Jarvinen TL, Jarvinen M. Organization and distribution of intramuscular connective tissue in normal and immobilized skeletal muscles. An immunohistochemical, polarization and scanning electron microscopic study. J Muscle Res Cell Motil. 2002;23:245–54. doi: 10.1023/a:1020904518336. [[DOI](#)] [[PubMed](#)] [[Google Scholar](#)]

24. Shiffman C, Aaron R, Altman A. Spatial dependence of the phase in localized bioelectrical impedance analysis. Phys Med Biol. 2001;46:N97–104. doi: 10.1088/0031-9155/46/4/402. [[DOI](#)] [[PubMed](#)] [[Google Scholar](#)]

25. Rutkove SB, Caress JB, Cartwright MS, et al. Electrical impedance myography as a biomarker to assess

ALS progression. Amyotrophic Lateral Sclerosis. 2012;13:439–45. doi: 10.3109/17482968.2012.688837. [\[DOI\]](#) [\[PMC free article\]](#) [\[PubMed\]](#) [\[Google Scholar\]](#)

26. Tarulli A, Esper G, Lee K, Aaron R, Shiffman C, Rutkove S. Electrical impedance myography in the bedside assessment of inflammatory myopathy. Neurology. 2005;65:451–2. doi: 10.1212/01.wnl.0000172338.95064.cb. [\[DOI\]](#) [\[PubMed\]](#) [\[Google Scholar\]](#)

27. Hortobagyi T, Houmard JA, Stevenson JR, Fraser DD, Johns RA, Israel RG. The effects of detraining on power athletes. Med Sci Sports Exerc. 1993;25:929–35. [\[PubMed\]](#) [\[Google Scholar\]](#)

28. Bevier WC, Wiswell RA, Pyka G, Kozak KC, Newhall KM, Marcus R. Relationship of body composition, muscle strength, and aerobic capacity to bone mineral density in older men and women. J Bone Miner Res. 1989;4:421–32. doi: 10.1002/jbmr.5650040318. [\[DOI\]](#) [\[PubMed\]](#) [\[Google Scholar\]](#)

29. Allen DL, Yasui W, Tanaka T, et al. Myonuclear number and myosin heavy chain expression in rat soleus single muscle fibers after spaceflight. Journal of applied physiology. 1996;81:145–51. doi: 10.1152/jappl.1996.81.1.145. [\[DOI\]](#) [\[PubMed\]](#) [\[Google Scholar\]](#)

30. Harrison BC, Allen DL, Girten B, et al. Skeletal muscle adaptations to microgravity exposure in the mouse. Journal of applied physiology. 2003;95:2462–70. doi: 10.1152/japplphysiol.00603.2003. [\[DOI\]](#) [\[PubMed\]](#) [\[Google Scholar\]](#)

31. Narici MV, de Boer MD. Disuse of the musculo-skeletal system in space and on earth. Eur J Appl Physiol. 2010;111:403–20. doi: 10.1007/s00421-010-1556-x. [\[DOI\]](#) [\[PubMed\]](#) [\[Google Scholar\]](#)